Fermilab

TM-584
2100.000

THE POTENTIAL PHYSICS PROGRAM OF THE 168-IN. HEPL FOCUSSING SPECTROMETER AT FERMILAB

Z. G. T. Guiragossian
High Energy Physics Laboratory
Stanford University, Stanford, California

and

A. L. Read
Fermi National Accelerator Laboratory
Batavia, Illinois

May 1975

INTRODUCTION

In this paper we discuss the potential physics research program that could be done at Fermilab with the use of the (at present partially constructed) HEPL 168" focussing spectrometer. We begin with a brief description of the spectrometer itself, followed by discussion of two distinct class of experiments that could be done. In the first class, the spectrometer would be used as a "stand-alone" device, that is, as a single-arm spectrometer, to study hadron-hadron and electron-hadron elastic scattering and inclusive deep inelastic scattering of hadrons, electrons and photons, on protons and deuterons, over a wide range of kinematic variables. For the second series of experiments, the spectrometer would be used as a highly selective trigger device in the study of a wide variety of exclusive channels in high energy hadron-hadron, electron-hadron, and photon-hadron scattering. In such experiments, a downstream spectrometer - such as the spectrometer described in Fermilab Proposals 192 and 193 - would identify and measure additional high-momentum collision products, in coincidence with the 168" spectrometer. The principal thrust of this paper is to discuss the physics potential of the 168" spectrometer; we do not describe here such matters as costs, schedules, details of experimental facility requirements, and other such (important!) logistical factors.

The 168" Focussing Spectrometer

The 168" focussing spectrometer[1] can be simply characterized as a scaled-up version of the HEPL 72" spectrometer, which was used for many years in a highly successful series of electron scattering

experiments at the Mark III Stanford electron linac. The principal performance characteristics which were specified for the 168" spectrometer are shown in Table I. Also, Fig. 1 displays elevation views of the spectrometer with its support structure and shielded detectors hut. The magnet is designed to have a field gradient index of $n = \frac{1}{2}$ which provides double focussing, on a point-to-point basis, with unit optical magnification. If desired, it is possible to have other magnification values. Unit optical magnification is obtained by having a source point (the target) always located a distance of 117.74" away from the magnet entrance aperture and also, by placing detectors a distance of 117.74" away from the magnet exit aperture. At that location, the momentum focal plane is tilted away from the normal to the optical axis by 54.74°. Track momenta and target exit coordinates are measured by a MWPC positioned on this plane; θ and ϕ angles are measured by MWPC's located ahead and behind the tilted focal plane, with lever arms of 20-25 feet. The shielded detectors hut extends out, over the bridge-type superstructure, providing a distance of 29 feet beyond the focal plane. This area would be used to accommodate two gas threshold Cerenkov counters, MWPC's, dE/dx counters, time-of-flight counters and total absorption counters, for identification (of e, μ, π, k, p, d and α particles) in the range 0.2 - 2.5 GeV/c.

The focussing spectrometer requires a floor space area of about 70' x 70' to allow for the spectrometer rotation between 28° and 152°, together with a bridge-construction type of support structure (see Fig. 1), which houses the detectors in a shielded

area. The detectors are located 28' above beam height and the detectors hut is 42' from the floor. Thus, a ceiling height of about 50' is needed. An experimental area might be planned in such a way as to accommodate this facility, followed by a space about 40' wide and 130' long for the installation of forward (i.e., downstream) spectrometer (s) and detectors. A possible location for this entire installation would be the secondary beam facility in the Proton-West beam area.

Potential Physics Program

The potential physics program of the 168" focussing spectrometer will be described in terms of two general configurations.

a) In the simpler case, the spectrometer would be used exclusively as a "stand-alone" device to provide precise knowledge on the behavior of elastic and quasi-two-body scattering processes and on the missing mass spectra in deep inelastic hadron-hadron, electron-hadron and photon-hadron scattering.

b) In a more complete arrangement, the focussing spectrometer would be used together with a large acceptance forward spectrometer arrangement consisting of large aperture magnets, MWPC's, cells of threshold gas Cereknov counters and total absorption counters made up of Pb-glass or NaI modules, in order to study details of specific "exclusive" reaction channels.

The 168" spectrometer would be capable of operating at incident beam intensities as high as 10^{13} p/pulse, since all of the experimental detectors associated with the spectrometer would be mounted some 30' above the beam line in a well shielded environment. Thus, it would be possible to do particle search experiments

with very good mass and momentum transfer resolutions and very high statistics in a reasonable length of running time. If new or anomalous effects were observed in a "stand-alone" search experiment, the role of the spectrometer would change from being a "search" device to becoming a "trigger" device for utilization with a forward spectrometer configuration. In this way, the forward spectrometer configuration would be triggered in a highly selective fashion in order to study details of a specific reaction channel or a new phenomenon.

I. Physics with the "Stand-Alone" 168" Focussing Spectrometer

Elastic Scattering

Hadron-hadron elastic scattering cross sections could be measured to obtain the differential cross sections $d\sigma/dt$ with high statistics and very narrow 'binning' in the momentum transfer range from $-t = 0.040$ GeV^2 to $-t = 3.3$ GeV^2.

Let us consider the rate of detected events in the dip structure region at $-t \sim 3.0$ GeV^2, for πp elastic scattering: (we assume πp elastic scattering has a dip and that the cross section at the dip is the same as in pp elastic scattering).

$$\frac{d\sigma}{dt} \approx 10^{-31}\ \mathrm{cm}^2/\mathrm{GeV}^2$$

From Table IV, the acceptance range of the spectrometer in t, including azimuthal acceptance, is $\Delta t = 0.03$ GeV^2, so that $\Delta\sigma \approx 3 \times 10^{-33}$ cm^2 would be the smallest cross section to be measured

in this experiment. We assume a target length of 20 cm (LH_2) and 10^9 particles/pulse; then the event luminosity is 3×10^{-33} $cm^2 \times 10^{33}$ cm^{-2}/pulse = 3/pulse at $t \simeq 3.0$ GeV^2 for πp elastic scattering, from a pion beam of 10^9/pulse, and 300 events/pulse at $t \simeq 3.0$ GeV^2 for pp elastic scattering, from a proton beam of 10^{11}/pulse. Event acquisition rates would be limited electronically to $\sim 10^3$ events/pulse.

Beam Requirements

The 168" spectrometer facility would be placed at the end of a beam line which provides both full-energy protons and also secondary particles at the highest energies and intensities planned at Fermilab. This might well be the currently evolving Proton-West secondary beam.

Bradley Cox has designed this beam, using superconducting elements; high-order aberrations are corrected by sextupoles. It should be possible to have the following secondary beam intensities and momentum ranges:

Attenuated protons	10^{10} - 10^{11}/pulse	50 - 1000 GeV/c
π	10^8 - 10^{10}/pulse	50 - 800 GeV/c
pure electrons	10^8 - 10^{10}/pulse	50 - 700 GeV/c
K^-	10^6 - 10^7 /pulse	50 - 700 GeV/c
antiprotons	10^6 - 10^7 /pulse	50 - 700 GeV/c
broad-band pure photons 1/2	10^8 - 10^{10}/pulse	50 - 700 GeV/c

Appropriate optical properties of the beam would be as follows:

1) beam angular definition: $\Delta\theta = \Delta\phi \leq \pm \frac{1}{4}$ mrad
2) horizontal spot size: $\Delta x = \pm 1$ mm
3) vertical spot size: $\Delta y = \pm 1$ mm
4) beam momentum definition: $\Delta p/p = \pm 1\%$

The Proton-West secondary beam, as presently planned, could fulfill these requirements. Antiproton and kaon tagging would be done by threshold Cerenkov counters in the beam.

A pure beam of electrons can be obtained by the use of a scheme in which the synchrotron radiation energy loss of electrons would be utilized to great advantage as the beam passed through the superconducting beam transport dipoles.

From the pure electron beam (Z. G. T. Guiragossián, HEPL report in preparation) with intensity of ~ 10^9 e/pulse, a broad band pure photon beam is produced by the use of a 1/3 r. l. Pb radiator. The radiator would be placed some 20' ahead of the charged beam focus, a sufficient distance to allow for bending of the electrons into a beam dump. For example, from 200 GeV 10^9 e/pulse, the number of photons in the range of 50 GeV to 200 GeV would be

$$\gamma/\text{pulse} = 1/3 \times 10^9 \times \ln (200/50) \simeq 0.5 \times 10^9\ \gamma.$$

The 200 GeV 10^9 e/pulse would be produced from a 400 GeV primary beam with intensity 10^{13} p/pulse. One can compare this yield of pure gamma-rays to that found in the Proton-East broad-band 0°

neutral beam where a measurement gives 2×10^7 $\gamma/10^{13}$ p/pulse in the range of 50 GeV to 200 GeV, from 300 GeV protons. We see that the Proton-West hadron/electron beam could produce a photon beam with substantially higher intensity and with excellent purity. The details of the γ beam proposal are described elsewhere.[2]

The desired optical properties of the beam, when it is used in conjunction with the 168" spectrometer, were determined from the following considerations.

1) Although the inherent angular resolution of the spectrometer is ± 0.1 mrad, multiple scattering of recoil particles in the LH_2 target degrades this resolution (typically, ± 0.25 mrad, for momentum of 1 GeV/c). The beam angular divergence should be comparable with or smaller than, the measurement error caused by the multiple scattering in LH_2. This beam divergence can be accomplished with the use of aperture stops placed at appropriate places along the secondary beam line.

2) The horizontal spot size of the beam determines the magnitude of the uncertainty in the energy-loss correction for slow recoil particles from the LH_2 target. A spot size of ± 1 mm corresponds to maintaining the inherent momentum resolution of the spectrometer, for recoil momenta above 1 GeV/c.

3) Because the spectrometer bends vertically, the vertical spot size of the beam is imaged at the (tilted) momentum focal plane of the spectrometer. A distance of 1.7 mm in this plane corresponds to 0.01% in momentum. The focal plane is tilted 54.74° away from the normal to the optical axis. Thus, a vertical spot size of ± 1 mm is needed, in order to preserve the inherent momentum resolution of the spectrometer.

4) In a missing-mass experiment, the uncertainty in missing-mass caused by uncertainty in beam momentum determines the maximum allowable beam momentum spread. Typically, a beam momentum definition of ± 1% would be appropriate; this could be accomplished by the use of a combination of aperture stops and momentum slits in the secondary beam line.

The target length acceptance of the spectrometer has a trapezoidal shape with a flat-top about 5" long, for scattering angles near 90°; longer targets can be used at angles far above or far below 90°. A typical target length might be 20 cm. The spectrometer would rotate about the target with a rotation arm equal in length to the focal length of the spectrometer; this is given approximately by $F = R/\sqrt{2}$ where R = 168" is the bending radius. The exact focal length is 117.74". A vacuum chamber extends out of the magnet by a length of 110" to eliminate multiple coulomb scattering in this region. The same vacuum chamber continues through the magnet and extends some 30" out of the magnet at the top. At unit optical magnification, the tilted focal plane is located 117.74" away from the exit aperture of the magnet. Detectors can be placed ahead of, at, and beyond, this focal plane. The magnet can be set at scattering angles from 28° to 152° without obstruction of the primary beam by the magnet support structure.

A liquid hydrogen or deuterium target would be used, in the form of a cylindrical tube 3 mm in diameter and 20 cm long. The beam spot occupies 2 mm in diameter. Target windows could be made of 1 mil thick Beryllium alloy sheets[3], as would the thin windows of the magnet vacuum chamber. This is a commercially

available material and the technology of making special flanges for windows using this material has been developed[3]. If one used such a target, the principal multiple scattering effects would be due entirely to the liquid hydrogen or deuterium itself.

The rms uncertainty in angle and momentum due to such multiple scattering effects is given by

1) $\Delta\theta_{ms} = 0.195 \text{ MeV}/c/p\beta$

2) $(\Delta p/p)_{ms} = (dE/dx) \cdot (0.1 \text{ cm})/p\beta$

where p in MeV/c is the recoil particle momentum and βc is its velocity; dE/dx in MeV/cm is the ionization energy loss of the recoil particle at a given momentum p.

The missing mass resolution depends on the uncertainties in beam momentum, p_1, in recoil particle momentum p_3, and recoil particle angle θ_3. We use the notation:

$$\vec{p}_1 + \vec{p}_2 \rightarrow \vec{p}_3 + \overrightarrow{MM} \text{ (momenta)}$$

$$m_1 + m_2 \rightarrow m_3 + M \quad \text{(masses)}$$

The following equations define the contributions of the various errors to the missing mass resolution:

$$(3) \quad \Delta M_{p_1} = p_1 \left[p_3 \cos\theta_3 - (E_3 - m_2)\beta_1\right]/M \times (\Delta p_1/p_1) = f_{p_1} \times \frac{\Delta p_1}{p_1}$$

$$(4) \quad \Delta M_{p_3} = p_3 \left[p_1 \cos\theta_3 - (E_1 + m_2)\beta_3\right]/M \times (\Delta p_3/p_3) = f_{p_3} \times \frac{\Delta p_3}{p_3}$$

$$(5) \quad \Delta M_{\theta_3} = p_1 p_3 \sin\theta_3/M \times (\Delta\theta_3) = f_{\theta_3} \times \Delta\theta_3$$

The overall missing-mass uncertainty is the quadratic sum of the above three terms.

At high energies, the kinematical factors in these equations are such that f_{p_1} is about 200 times smaller than f_{p_3}, and f_{p_3} is about 2 - 3 times smaller than f_{θ_3}. Typical values of these factors are given in Tables II and III. This means that a 1% beam momentum definition is more than sufficient to match with the 0.01% definition of the recoil particle momentum; the contribution from equation (3) is negligible and the dominant term is equation (5).

In Table II we show values of missing-mass resolution for the cases of 300 GeV/c and 900 GeV/c pp elastic scattering where the measurement would be made with ~ 1% beam momentum bite. For example, at 300 GeV/c and at momentum transfer values of $-t = 1.0 \rightarrow 3.1\ \mathrm{GeV}^2$ the missing-mass resolution is 60 MeV; the missing-mass acceptance is a few GeV wide. Here, elastic events can be selected with extremely good precision while measurements are being made simultaneously on quasi-two-body reactions to study production of excited baryons.

As is seen in equations (3) - (5) the missing-mass resolution improves at larger mass values by the factor 1/M. In Table III

we give values of missing-mass resolution for the case of 300 GeV/c deep inelastic $\pi^- p$ scattering. For example, the mass region around 10 GeV can be studied with a mass acceptance of about 2 GeV (FW) and with missing-mass resolution of 5 MeV.

Finally, in Table III and IV we give the acceptance and resolution of the momentum transfer variable, t. We use the equation

$$(6) \quad \delta t = 2m_2 \, p_3^{\,2}/E_e \cdot (\delta p_3/p_3)$$

for the resolution in t. The acceptance in t, including the azimuthal acceptance of the spectrometer, is given by:

$$(7) \quad \Delta t_{accept} = (dt/d\Omega) \cdot \Delta\Omega_{accept}; \; \Delta\Omega_{accept} = 0.012 \text{ sterad.}$$

The dependence of $dt/d\Omega$ on the measured variables p_3 and θ_3 is:

$$(8) \quad \frac{dt}{d\Omega} = \frac{2m_2 \, p_1 p_3^{\,3}}{\pi} \times \frac{1}{\left[(M^2 - m_3^{\,2} - s)\, E_3 + 2m_3^{\,2}\,(E_1 + m_2)\right]}$$

where the missing-mass M, is obtained by:

$$(9) \quad \cos\theta_3 = \frac{M^2 - m_3^{\,2} - s + 2E_3(E_1 + m_2).}{2p_1 p_3}$$

We see that the resolution in t is in most cases $\sim 10^{-4}$ GeV^2.

Deep Inelastic Scattering (missing-mass search mode)

Missing-mass search type experiments have been productive in discovering new states of heavy baryons and bosons: Resolution in missing mass is crucial because usually such states are observed in the presence of a large background continuum; also, the states may have narrow line widths.

Let us consider the following reactions:

a) $pp \to p + M_x^+$ (for heavy baryons, etc.)

b) $\pi^- p \to p + M_x^-$ (for heavy mesons, etc.)

c) $ep \to p + M_x$ (for excited leptons, heavy leptons, etc.)

d) $\gamma p \to p + M_x^o$ (for heavy vector bosons)

Figure 2 shows the kinematical region covered in terms of the Feynman scaling variables $p_\perp$ and x ($x = 2p_\parallel^*/\sqrt{s}$). The top figure is for the case where recoil protons are accepted in the spectrometer, and equivalently, the bottom figure is where recoil pions are accepted. In each figure, the phase space region in $p_\perp$ and x covered by the spectrometer is indicated by the shaded boundaries.

In Table III several parameters for reaction (b) are listed for missing-mass values of 5, 10 and 15 GeV, for a pion beam at 300 GeV/c. A typically small cross section, say at $p_\perp = 1.8$ GeV/c and x = -1, is estimated to be approximately

$$\frac{d^2\sigma}{d\Omega dp} \sim 0.1 \text{ mb/sr} \cdot \text{GeV/c}.$$

Let us estimate the total cross-section within the spectrometer acceptance. We find:

$$\Delta\Omega \cdot (\Delta p/p) \cdot p = 0.0116 \text{ (sr)} \times 0.112 \times 2.5 \text{ GeV/c}$$
$$= 0.32 \cdot 10^{-2} \text{ (sr} \cdot \text{GeV/c)}$$

for the case of $p = 2.5$ GeV/c and $\theta = 45^{\circ}$. Thus $\Delta\sigma_{accept} = 0.3 \cdot 10^{-30}$ cm^2, and with a luminosity of $0.8 \cdot 10^{33}$ cm^{-2}/pulse, corresponding to 10^9 pions/pulse on a 20 cm LH_2 target, we obtain 250 events/pulse.

We see that the above four reactions can be studied with good statistics. In the case of a proton beam, 10^{10} p/pulse appears to be sufficient to saturate maximum data collection rates. 10^8 - 10^9 π/pulse will give 25 - 250 events/pulse in the region of low cross-sections. Also, 10^8 - 10^9 electrons/pulse would be available in the P-West secondary beam. If we assume the electron reaction rates to be 1/1000 that of the corresponding pion reaction rates we would expect minimum rates of 0.025 - 0.25 events/pulse in this kind of experiment. The elastic ep cross-section at $q^2 = 3$ GeV^2 is 10^{-34} cm^2/GeV^2 at 200 GeV so that $\sigma_{accept} = 0.3 \cdot 10^{-35}$ cm^2, yielding 1 event/hour. At $q^2 = 0.7$ GeV^2, the rate is 1 event/pulse. We summarize this section of our report by listing the reactions of interest in the "stand-alone" mode of operation. We consider rates of interest to be 0.02 events/pulse at the lowest, corresponding to 1 event in 10 minutes, and 1000 events/pulse at the highest. (The first named of the two outgoing particles, in each of the reactions listed on the following page, is the one which is accepted by the spectrometer).

a) Elastic (forward)

1. $pp \rightarrow pp$
2. $\pi^- p \rightarrow p\pi^-$
3. $\bar{p}p \rightarrow p\bar{p}$
4. $K^- p \rightarrow pK^-$
5. $e^- p \rightarrow pe^-$

b) Elastic (backward)

6. $\pi^- p \rightarrow \pi^- p$
7. $\bar{p}p \rightarrow \bar{p}p$
8. $K^- p \rightarrow K^- p$

c) Quasi-Two-body

9. $pp \rightarrow pN^{*+}$, (baryon resonances)
10. $\pi^- p \rightarrow p\pi^{*-}$, (meson resonances)
11. $\pi^- p \rightarrow K^+ Y^{*-}$ (hyperon resonances)
12. $e^- p \rightarrow pE^{*-}$ (possible heavy leptons)

High statistics and good resolution are important if one wants to be able to unravel possible fine structures in the differential angular distributions in a reasonably finite period of running time.

II. Physics with the 168" and a Forward Spectrometer

A forward spectrometer can be used operating in coincidence with the 168" focussing spectrometer for the purpose of acquiring detailed knowledge on the production of specific "exclusive" final states. The forward spectrometer must be able to operate at quite high beam intensities, in order to match well with the capabilities

of the recoil focussing spectrometer. An example of such a forward spectrometer is given in the proposal of Fermilab experiment E-192, in which large angle particle pairs will be detected and identified for the cases of gamma-rays, electrons, muons and hadrons.

In the two-spectrometer arrangement we have outlined, the forward spectrometer would be used to study details of the production and decay of massive states of fermions and bosons. There are many possible such experiments. We mention a few representative examples:

a) $\pi^- p \to pM;\ M^- \to \pi^-\pi^o$

b) $\gamma p \to p\psi;\ \psi \to e^+e^-$

c) $pp \to pN^{*+};\ N^{*+} \to p\pi^o$

d) $ep \to pE^{*-};\ E^{*-} \to e^-\gamma$

In all of these cases, the mass acceptance is limited by the focussing spectrometer since one can certainly build a forward particle pair spectrometer which has a very wide mass acceptance at a uniform efficiency of a few percent (see for instance, the E-192 arrangement).

We define a detection sensitivity in terms of B, the decay branching ratio, multiplied by the double differential cross-section $d^2\sigma/dMdt$ for a given one of these reactions. The luminosity on a 20 cm LH_2 target could be 10^{33} cm^{-2}/pulse or higher. From Table III, we have acceptances ΔM = 4 GeV and Δt = 0.0165 GeV^2, (including the azimuthal acceptance of the 168" spectrometer) in the t range of 1.5 - 2.0 GeV^2, for a particle mass of 5 GeV. The forward spectrometer has typically an azimuthal acceptance of $\frac{f_\phi}{2\pi} = 0.02$. Thus,

we give a sensitivity figure based on the detection of 100 events in a 100 hour run, at 500 pulses/hour in 400 GeV accelerator operations:

$$100 \text{ events} = B \frac{d^2\sigma}{dMdt} \cdot$$

$$(4 \text{ GeV}) \cdot (0.0165 \text{ GeV}^2) \cdot 0.02 \cdot 10^{33} \text{ cm}^{-2}/\text{pulse} \cdot (100 \text{ hours}) \cdot (600 \text{ pulses/hour})$$

$$B \frac{d^2\sigma}{dMdt} = 1.3 \cdot 10^{-33} \text{ cm}^2/\text{GeV}^3.$$

Compared with other search type experiments, even though there is in this case a restriction in event-rate which is introduced by the finite azimuthal acceptance of the recoil spectrometer, this method seems to be a competitive search tool since it possesses the important characteristics of very fine binning both in "forward-system mass and in "momentum transfer to forward system".

[1]Z. G. T. Guiragossián and R. Hofstadter, "Technical Description of the HEPL 168" Focussing Spectrometer," HEPL-Report No. 754 (1975).

[2]Z. G. T. Guiragossián, "50 - 800 GeV, 10^8 - 10^{10} Pure Electron and Broad-Band Photon Beams at FERMILAB," HEPL-Report No. 756 (1975).

[3]Thin Beryllium sheets are supplied by Beryllco and Brush Beryllium companies. The technology of making Beryllium window flanges has been developed at the Lawrence Livermore Laboratory.

TABLE I

CHARACTERISTICS OF THE 168" HEPL 2.5 GeV/c HIGH RESOLUTION LARGE ACCEPTANCE SPECTROMETER

Optics	point-to-point double focussing, n = 1/2 magnet, unit magnification
Target length	13 cm target acceptance at $\theta = 90^{\circ}$ (flat top of distribution); 39 cm acceptance full length (at base of distribution).
Maximum momentum	2.5 GeV/c
Solid angle acceptance	11.6×10^{-3} strad.
Horizontal angular acceptance	44 mrad.
Vertical angular acceptance	264 mrad.
Momentum acceptance	11.12% (FW)
Momentum resolution	10^{-4}
MWPC spatial resolution required to match momentum resolution	± 1.7 mm
MWPC spatial resolution actually available	± 0.6 mm
Production angular resolution	± 0.1 mrad.
Power requirement	2 MW at p_{max} = 2 GeV/c 3.7 MW at p_{max} = 2.5 GeV/c
Total spectrometer turning radius	32'6"; 9.9 m
Beam line height from supporting floor	6'6"; 1.98 m
Total spectrometer height from supporting floor	46' ; 14 m
Magnet weight	1100 tons; 1010 metric tons
Magnet superstructure weight	300 tons; 272 metric tons

TABLE II

300 GeV/c pp Elastic			f_{p_1} (GeV)	f_{p_3} (GeV)	rms Momentum error	f_{θ_3} (GeV)	rms Angle error	(MeV)	(MeV)	(MeV)
p_3	θ_3	t	$\Delta M_4/\Delta p_1/p_1$	$\Delta M_4/\Delta p_3/p_3$	$\Delta p_3/p_3 \cdot 10^{-4}$	$\Delta M_4/\Delta\theta_3$	$\Delta\theta_3 \cdot 10^{-4}$	$\Delta M_4)_{p_3}$	$\Delta M_4)_{\theta_3}$	ΔM_4
536	74.55	0.267	0.1428	39.630	3.190	165.210	8.293	12.642	137.009	137.6
1486	56.44	1.537	0.8217	140.280	1.000	395.880	1.533	14.280	60.688	62.3
2404	46.74	3.084	1.6476	191.520	1.000	559.800	1.000	19.152	55.980	59.2

900 GeV/c pp Elastic			f_{p_1} (GeV)	f_{p_1} (GeV)	f_{θ_3} (GeV)	(MeV)	(MeV)	(MeV)
p_3	θ_3	t	$\Delta M_4/\Delta p_1/p_1$	$\Delta M_4/\Delta p_3/p_3$	$\Delta M_4/\Delta\theta_3$	$\Delta M_4)_{p_3}$	$\Delta M_4)_{\theta_3}$	ΔM_4
559	74.00	.289	0.1542	127.080	515.700	40.539	427.67	429.6
1509	56.20	1.573	0.8394	425.160	1202.670	42.516	184.37	189.2
2477	46.27	3.210	1.7124	581.850	1716.930	58.185	171.69	181.3

TABLE III

300 GeV/c $\pi p \to p$ + anything

MM = 5 GeV			(GeV)	(GeV)	(MeV)	(MeV)	(MeV)	(GeV)	$(GeV)^2$
MeV/c	p_3	θ_3	$\Delta m/\Delta p_3/p_3$	$\Delta m/\Delta\theta_3$	$\Delta M)_{p_3}$	$\Delta M)_{\theta_3}$	ΔM	ΔM_{accept}	$(dt/d\Omega)\Delta\Omega_{accept}$
	500	70.54°	4.157	28.286	1.326	23.458	23.5	1.33	0.0059
	1500	54.32°	24.046	73.106	2.405	11.207	11.5	4.18	0.0165
	2500	44.64°	34.202	105.398	3.420	10.540	11.1	6.00	0.0356

MM = 10 GeV			(GeV)	(GeV)	(MeV)	(MeV)	(MeV)	(GeV)	$(GeV)^2$
MeV/c	p_3	θ_3	$\Delta m/\Delta p_3/p_3$	$\Delta m/\Delta\theta_3$	$\Delta M)_{p_3}$	$\Delta M)_{\theta_3}$	ΔM	ΔM_{accept}	$(dt/d\Omega)\Delta\Omega_{accept}$
	500	54.32	1.672	12.184	0.533	10.104	10.1	0.57	0.0073
	1500	48.19	8.274	33.541	0.827	5.142	5.2	1.7	0.0240
	2500	40.40	13.326	48.609	1.333	4.861	5.0	2.6	0.0457

MM = 15 GeV			(GeV)	(GeV)	(MeV)	(MeV)	(MeV)	(GeV)	$(GeV)^2$
MeV/c	p_3	θ_3	$\Delta m/\Delta p_3/p_3$	$\Delta m/\Delta\theta_3$	$\Delta M)_{p_3}$	$\Delta M)_{\theta_3}$	ΔM	ΔM_{accept}	$(dt/d\Omega)\Delta\Omega_{accept}$
	1500	36.34°	1.349	17.777	0.135	2.725	2.73	0.80	0.0980
	2500	32.35°	4.718	26.755	0.472	2.676	2.72	1.29	0.0859

$(\Delta\theta_3)_{accept} = 0.044$ rad; $\Delta\Omega_{accept} = 0.0116$ sr; $(\Delta p_3/p_3)_{accept} = 0.112$

TABLE IV

MOMENTUM TRANSFER RESOLUTION AND ACCEPTANCE IN

$pp \rightarrow pp$ AND $\pi p \rightarrow p\pi$

GeV/c p_3	GeV^2 t	GeV^2 δt	GeV^2 $\Delta t_{accept} = (dt/d\Omega)\Delta\Omega_{accept}$
0.200	0.0396	0.00062	0.0014
0.500	0.2344	0.00014	0.0037
1.000	0.8125	0.00014	0.0085
1.500	1.5594	0.00024	0.0150
2.000	2.3849	0.00034	0.0232
2.500	3.2502	0.00044	0.0332

$\Delta\Omega$ = 0.0116 sterad

See Table II for rms $\delta p_3/p_3$

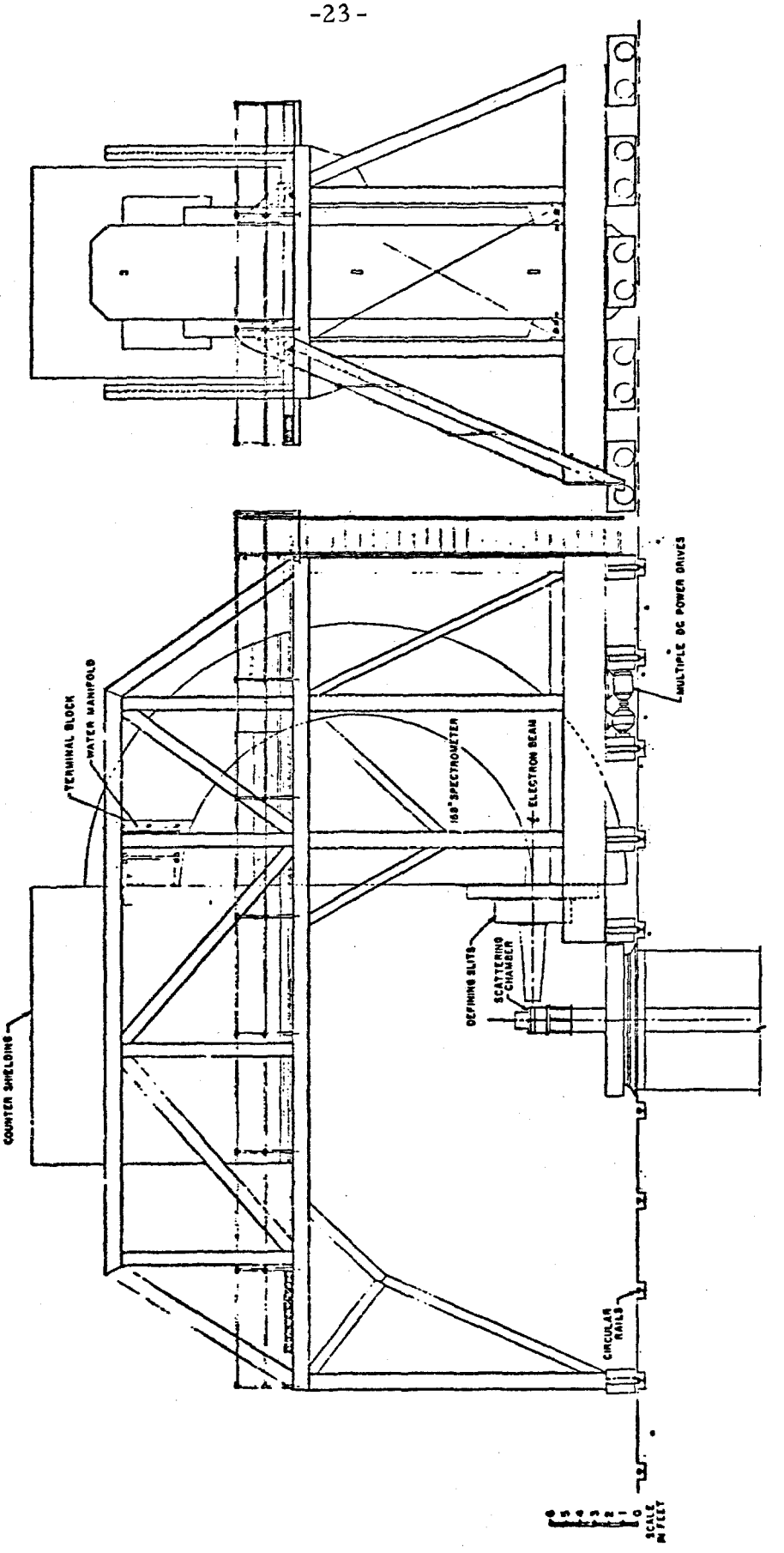
COUNTER SHIELDING
TERMINAL BLOCK
WATER MANIFOLD
180° SPECTROMETER
ELECTRON BEAM
DEFINING SLITS
SCATTERING CHAMBER
CIRCULAR RAILS
MULTIPLE DC POWER DRIVES
SCALE IN FEET

FIGURE 1

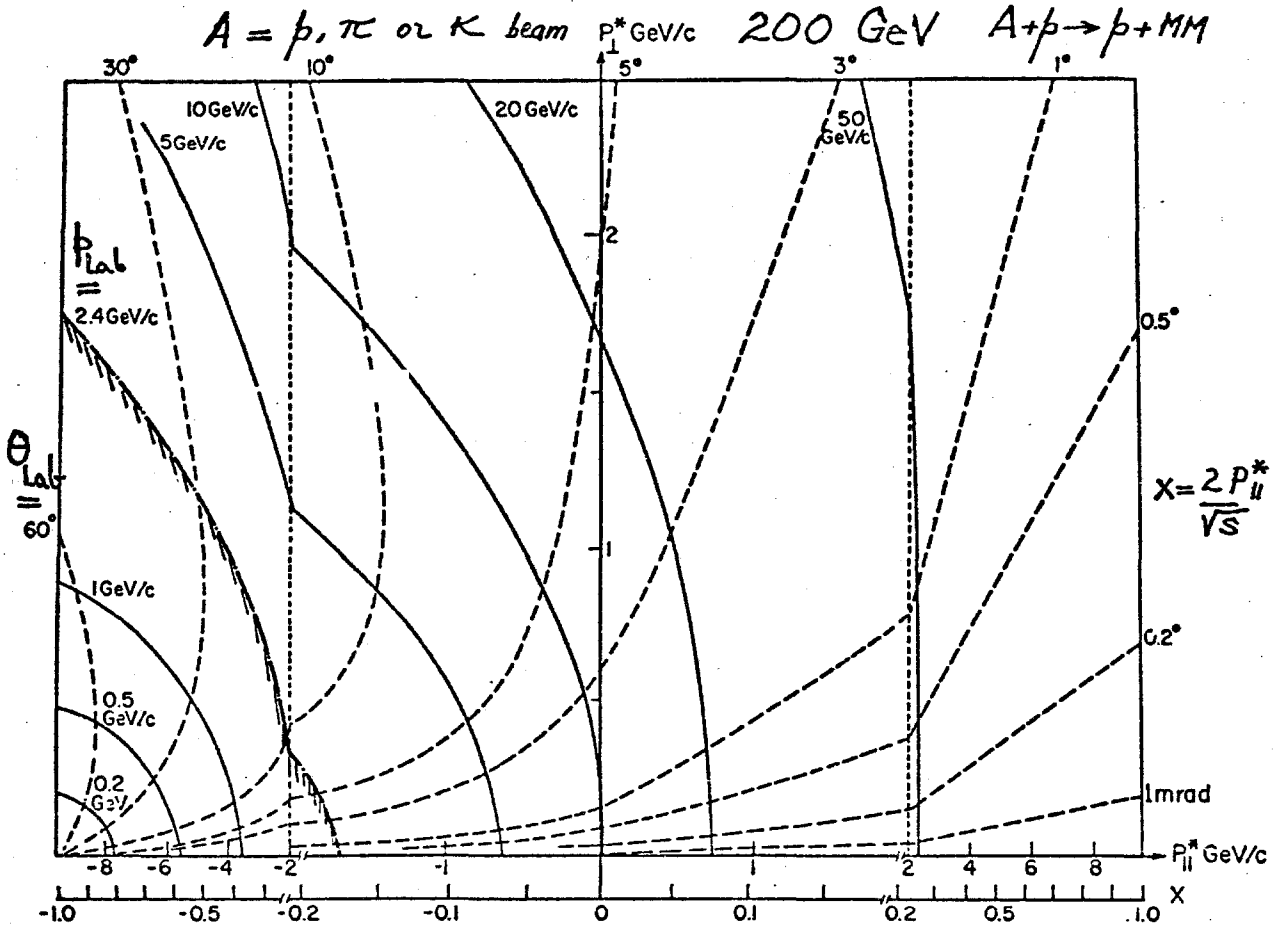
A = p, π or K beam
P*⊥ GeV/c
200 GeV
A+p→p+MM
30°
10°
5°
3°
1°
10GeV/c
5GeV/c
20GeV/c
50 GeV/c
p_Lab = 2.4GeV/c
θ_Lab = 60°
1GeV/c
0.5 GeV/c
0.2 GeV/c
0.5°
0.2°
1mrad
X = 2P*∥/√s
P*∥ GeV/c
X

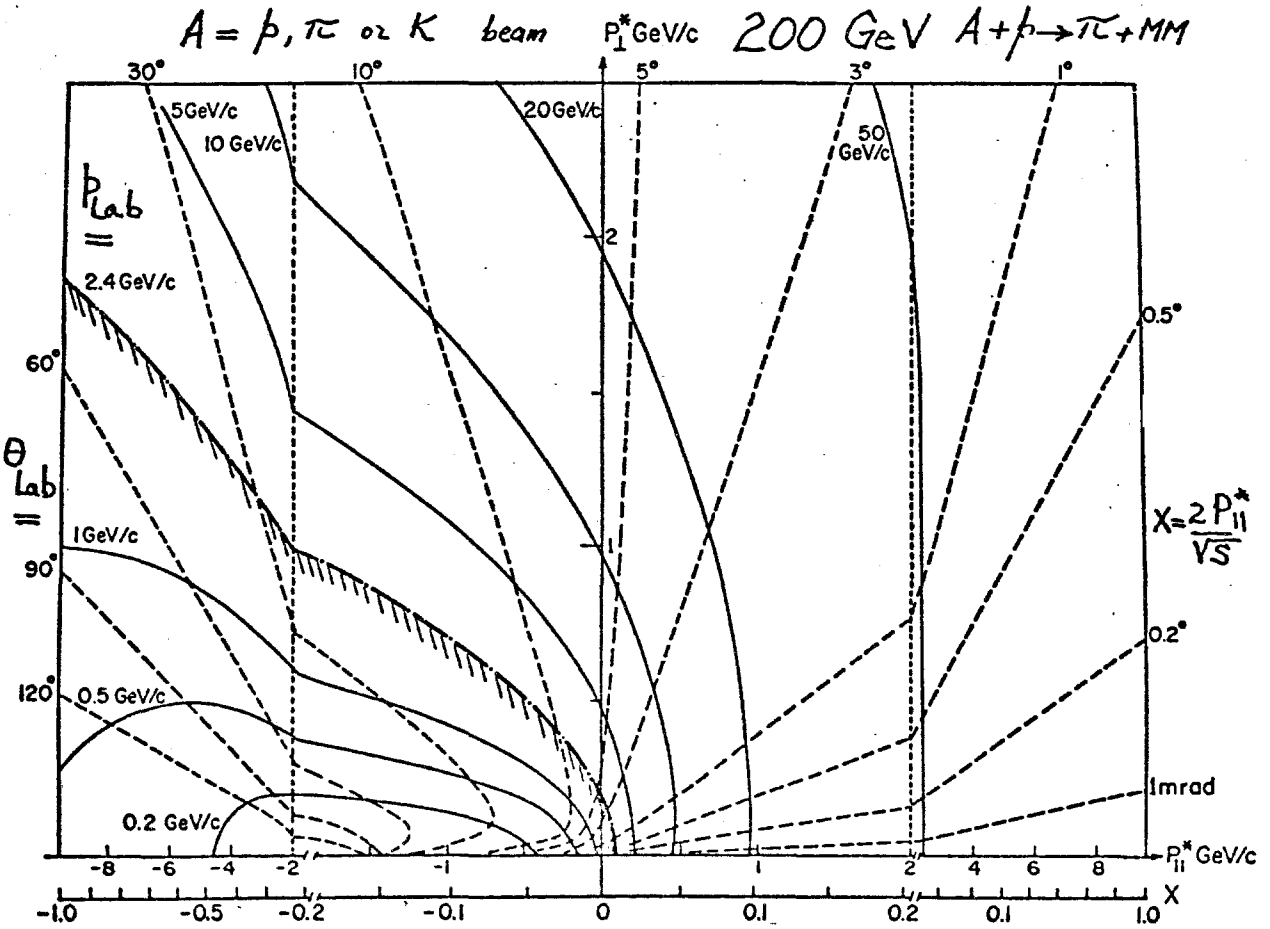
A = p, π or K beam
P*⊥ GeV/c
200 GeV
A+p→π+MM
30°
10°
5°
3°
1°
5GeV/c
10 GeV/c
20GeV/c
50 GeV/c
p_Lab = 2.4 GeV/c
θ_Lab = 60°
90°
120°
1GeV/c
0.5 GeV/c
0.2 GeV/c
0.5°
0.2°
1mrad
X = 2P*∥/√s
P*∥ GeV/c
X

FIGURE 2